

EFFECTS OF RADIATION PATTERN ON LOCAL SITE EFFECTS OF SEDIMENTARY BASIN

Kiyotaka SATO¹, Sadanori HIGASHI², Shunji SASAKI³ And Hiroshi YAJIMA⁴

SUMMARY

Total site effect evaluations based on geotechnical surveys and earthquake observation, make it possible to synthesize strong motion. The spectral ratios of the gravelly soil sediments at Kuno were constant in the S wave's predominant component corresponded to the focal radiation pattern. On the soft clay sediments at Takeyama, the spectral ratios to a reference point at the outcrop of bedrock were constant in accordance with seismic incident angle. Thus the site effects computed by analytical method agree with the observed spectral ratios by considering the incident wave field related to the source and path effects.

INTRODUCTION

Ashigara valley, Kuno (called AGK hereafter) is the international observation field for the ESG research group [IASPEI/IAEE, 1992]. Local site effects of two alluvial sedimentary basins at Kuno and at Takeyama (called TKY hereafter) in Miura peninsula were evaluated under strong motion array seismographs observation. AGK earthquake observation system was installed as a common project of all electric power industry, which are 9 electric power companies and Japan nuclear power cooperation. Some records were provided by Dr. Kazuyoshi Kudo, Earthquake Research Institute, University of Tokyo. We deeply appreciate all of them.

1.1 Gravelly soil sediments in AGK site

Fig.1 [Sato, K., 1998] shows those observation points and the schematic cross-section along the east to west line's profile for the reflection survey in the observation site.

AGK site and its vicinity have been explored to investigate velocity structure and physical properties of the subsurface structure. Logging provides valuable data for understanding geotechnical properties of soil deposits at downholes of AGK site. PS-logging has been carried out in downholes, called OA, OC to OF, at the depth from 20m to 330m. At a only OF point, the vertical seismic profiling (VSP) survey [Higashi, S., 1997] was also applied. Fig.2 shows schematic east to west cross section.

1.2 Soft clay buried valley in TKY site

TKY site is located on the middle part at the east shore of Miura peninsula and facing on the east of Sagami bay. Miura peninsula is based on Hayama group of old Tertiary. Miura and Sagami groups are distributed on upper layer of the Hayama group. On the basis of geological surveys in TKY site, it was confirmed that the rock of Miura group is outcrop at the west and Hayama group is distributed on the east. It was also recognized that this is a typical small sized buried valley along the west to the east.

As seen in Fig.3, P-wave seismic reflection surveys in shallow layer were carried out at 3-dimensional profiles. From these surveys, this site is just like a sedimentary basin, which is 300m wide and 25m deep. S-wave velocity structure on SG3 was obtained from PS logging as seen in Fig.4. S-wave velocities were ranging from 90 to 180

¹ Geotech & Earthq Eng Dept, Ctl Rsrch Inst Of Electric Power Ind. Abiko-shi, Chiba, Japan. E-mail ksato@abiko.denke.or.jp

²

³

⁴

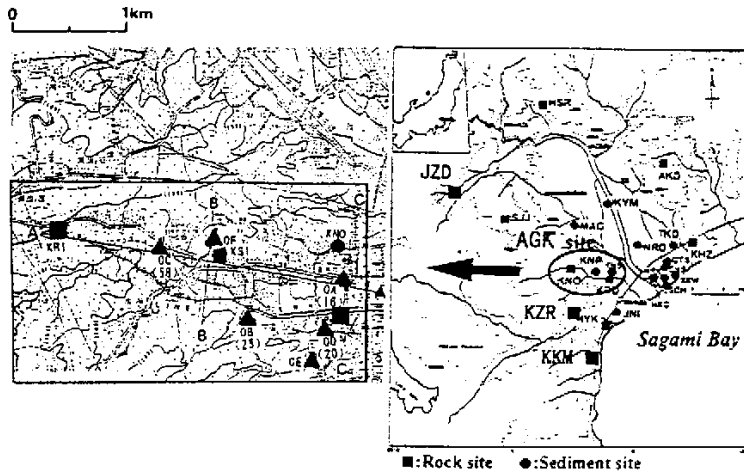


Figure 1: Magnified location map of observation area at AGK (▲ by EPCO, ● by CRIEPI, ■ by ERI)

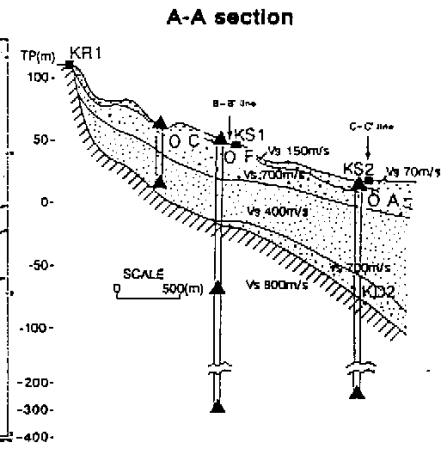


Figure 2: Schematic cross-section [IASPEI, 1992]

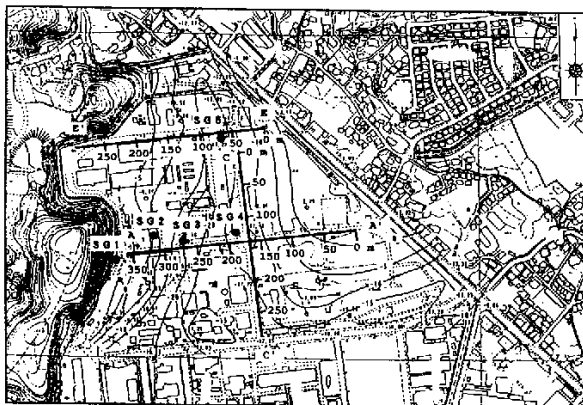


Figure 3: Location of observation area at TKY (Contour lines mean the depth of rock)

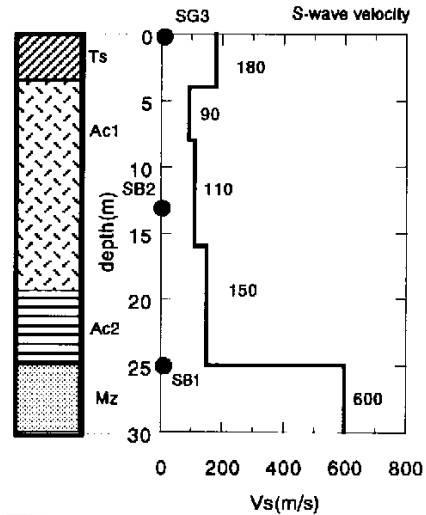


Figure 4: Geotechnical profile at TKY

m/s in Ac1 clay layer, 150 to 180 m/s in Ac2 clay layer for alluvial sedimentary basin, and 600 m/s in sandstone for bedrock.

2. FOCAL RADIATION PATTERN AND SEISMIC PATH EFFECT FOR SEISMIC RECORDS

Earthquake events were recorded from April in 1995 to November in 1997 as seen in Table 1 and Fig.5. Western Kanagawa earthquake (EQ.8) of these events is a near-field epicentral distance of 9.1km for AGK. The other earthquakes, Eastern Yamanashi (EQ.3a, 3b, 5a, 5b), East off Izu peninsula (EQ.6), Suruga bay (EQ.1) and Sagami bay (EQ.2) occurred in the region from about 20 to 60 km epicentral distance at surrounding locations of AGK. The magnitudes of those events were scaled from 3.9 to 5.7 and the focal depth was less than about 70km except EQ.2 at a depth of 122km. Even if large scaled earthquakes, such as EQ.3b and EQ.6, the length of those

Table1: Recorded earthquakes' property

EQ No.	Name of Earthquake	Date	Origin time	Latitude	Longitude	Depth (km)	Magnitude Mj	Epicentral distance from AGK (km)	Epicentral distance from TKY (km)
1	Suruga bay	1995/4/18	20:26	35° 03'	138° 35'	24	4.5	57.0	—
2	Sagami bay	1995/7/3	8:53	35° 09'	139° 34'	122	5.2	40.0	8.2
3a	E. Yamanashi	1996/3/6	23:12	35° 30'	138° 54'	16	4.3	34.5	—
3b	E. Yamanashi	1996/3/6	23:35	35° 30'	138° 54'	17	5.3	34.5	—
4	E. Off Chiba	1996/9/11	11:37	35° 38'	141° 12'	53	6.2	190.4	153.9
5a	E. Yamanashi	1996/10/25	12:25	35° 27'	139° 00'	23	4.5	24.6	61.7
5b	E. Yamanashi	1996/10/25	21:06	35° 28'	138° 59'	18	4.1	26.9	—
6	E. Off. Izu Penin.	1997/3/4	12:51	34° 10'	139° 10'	2	5.7	35.2	49.5
7	S. Ibaraki	1997/3/23	20:36	35° 58'	140° 06'	72	5.0	—	103.6
8	W. Kanagawa	1997/11/4	10:31	35° 12'	139° 06'	20	3.9	9.1	—

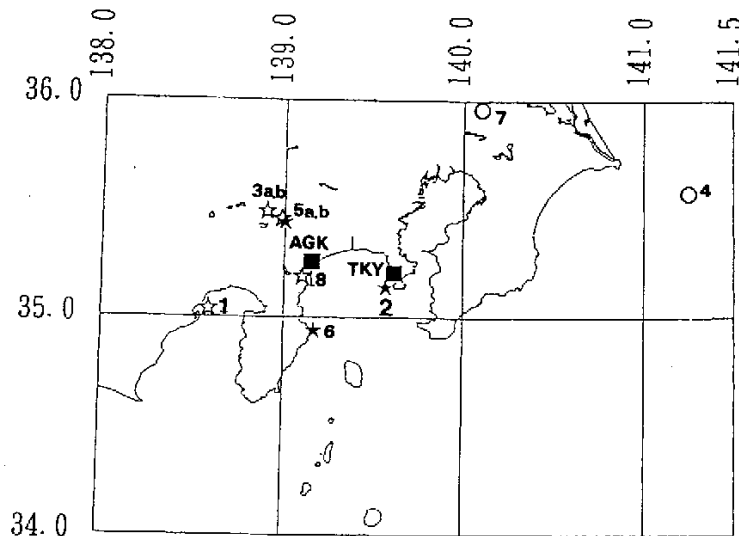


Figure 5: Analyzed seismic epicenter and observation locations

(☆:AGK record, ○:TKY record, ★:both sites record, ■:observation site)

faults obtained from the empirical equation estimated by Matsuda [1974] was smaller than the epicentral distance. So those events were identified as a point source with respect to AGK site as well as TKY site. EQ.2, EQ.5a and EQ.6 earthquakes were also observed at the same time in both sites. These events are about 50 to 60km epicentral distances except EQ.2 earthquake in the near field. On the other hand, South Ibaraki pref. (EQ.7) scaled $M_j=5.0$ and E. Off Chiba pref. (EQ.4) scaled $M_j=6.2$ are located in 104 km and 154 km to TKY.

2.1 Spectral ratios related to focal radiation pattern

First, the focal S-wave radiation patterns of those earthquakes were induced by moment tensor solution M_{pq} as a point source [Kennet, B.L.N., 1988]. The source parameters, such as a strike angle ϕ , dip angle δ and slip angle λ in the source fault estimated by the National Institute for Earth Science and Disaster Prevention (NIED) were obtained as seen in Table 2. The S-wave focal radiation patterns were given by moment tensor solution in those source parameters. It is a Green function, which induced the far-field displacement for a point source in a homogeneous medium.

The S wave radiation patterns for SH and SV waves were obtained on every 10 degrees at the azimuth and the take-off angles by using the above functions. Then the vectors were indicated as an equal area projection of the lower hemisphere of the focal sphere. The amplitude of vector is represented as ten steps from 0.1 to 1.0 every 0.1. The radiation patterns for every event were computed by the resolution of above moment tensor. Table 3 shows the azimuth and take-off angles to the OA observation point for each seismic source, based on the earth's

Table2: List of CMT solution for the analyzed seismic source
(by NIED:<http://www.bosai.go.jp/jindex.html>)

EQ.No	strike ϕ s(deg)	dip δ (deg)	slip λ (deg)	Magnitude Mj	depth h(km)
1	162.0	56.7	166	4.5	24
2	252.0	83.8	114	5.2	122
3b	24.3	50.0	102	5.3	20
4	132.0	63	-50	5.0	53
5a	207.0	35.0	90	4.5	23
6	69.8	58.2	-154	5.7	2
7	118.8	59.5	64.3	5.0	72
8	232.0	80.0	158	3.9	15

calaloged by NIED

Table3: Azimuth and take-off angles for AGK

EQ.No.	unit(degree)	
	OA	
	azimuth Φ	take-off θ
1	66	60
2	290	161
3b	139	118
5a	146	120
6	356	58
8	32	148

Table4: Azimuth, take-off and incident angles for TKY

EQ.No.	unit(degree)		
	SG1		
	azimuth Φ	take-off θ_o	incident θ_i
2	212	6	1.6
4	72	78	15.5
5a	295	85	17.9
6	234	58	22
7	28	59	13.6

crust structure [Yoshii, T., 1986] evaluated by artificial explosive seismic survey in Izu district. In the case of EQ.6, the SH wave's radiation pattern is predominantly larger than the SV wave's one as seen in Fig.6. In Fig.7, the S wave principal shocks are traced for the velocity seismograms at the surface of the sedimentary basin on OC, OF, and OA filtered by the Chebishev's band pass filter (BPF) at the range from 0.4 to 1.0Hz. In Fig.9, S wave's first motion of the velocity seismograms is apparently predominant in EW component much more than in NS component. It is coincided with the focal radiation pattern. In the case of EQ.8 and EQ.5a, the SV wave's radiation pattern is predominantly larger than the SH wave's one. The azimuth angle to OA from southwest direction in EQ.8 was 32 degrees and the azimuth angle from northwest in EQ.5a was 146 degree. So the S wave's first motions were predominant along both NS and EW components. But in EQ.3b, the S wave's principal axis was found to be inclined along EW direction of the sedimentary valley by the effect of the path process in the geological structure of Ashigara valley [Iligashi, S., 1998]. On the other hand, the SH wave's radiation patterns were so larger than the SV wave's ones in EQ.1 and EQ.2. Then the first S waves were predominantly larger in NS component than those in EW component. Those results of the seismograms mean that the S wave's principal axis is in response to the focal radiation pattern. The spectral ratios between the surface and bottom of downhole points were analyzed for the S wave's principal shock in horizontal components.

The groups of earthquakes were divided into NS and EW predominant due to the the S wave's focal radiation. EQ.1 and 2 are the NS predominant group. EQ.3b, 5a) and EQ.6 are EW predominant group. Only a EQ.8 belongs to both groups because the S wave's radiation is predominant along north-east directions.

As seen in a result of Fig.8 (a), the EW component spectral ratios appeared as constant characteristics in a low frequency region less than 2.5Hz in the EW predominant group. On the other hand as seen in Fig.8 (b), the EW component spectral ratios, of which peaks' amplitude were clearly fluctuated around 1Hz for every earthquake, apparently appeared as variable characteristics in the NS predominant group.

According to these results, it was clarified that the spectral ratios' property was constant in the low frequency region for the principal axis corresponded both to the focal radiation pattern and to path effect. So the site amplification on AGK is affected by both of the sedimentary basin and the incident wave field related to the source and path effects.

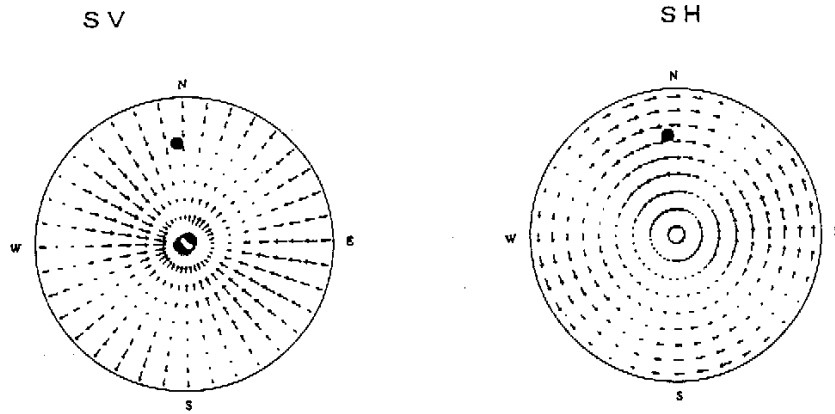


Figure 6: Focal radiation pattern of the lower hemisphere of the focal sphere for E. off Izu peninsula EQ.6 (Left: SV wave, Right: SH wave, ●: OA point)

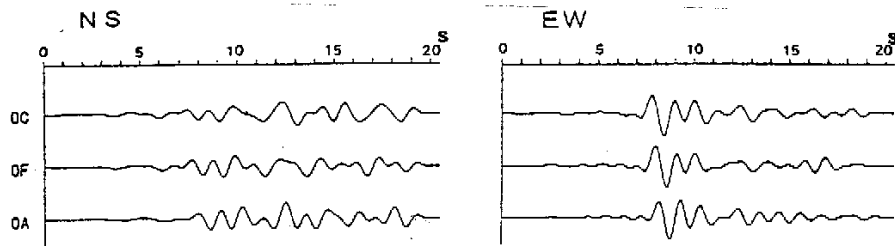
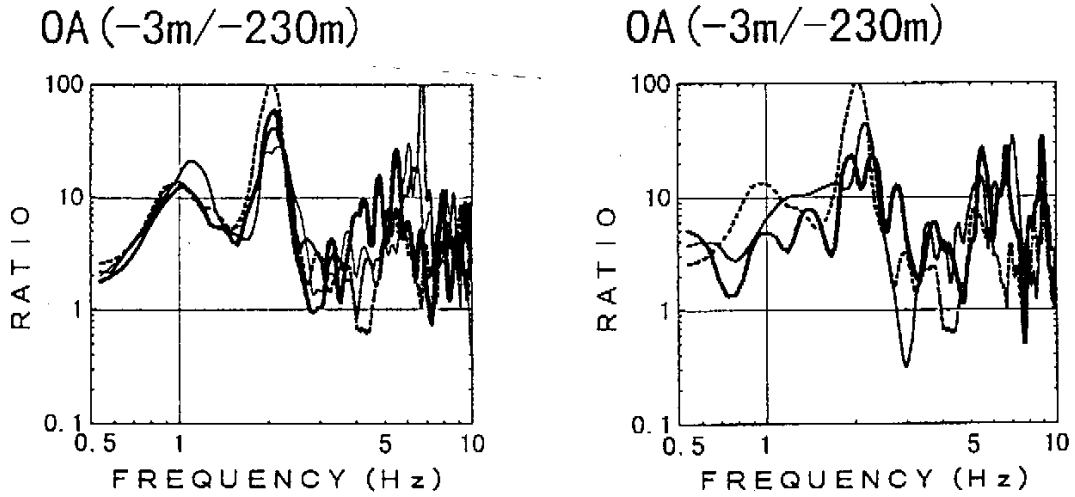


Figure 7: Horizontal BPF velocity seismograms on the AGK sediments (BPF range: 0.4 - 1.0Hz, EQ.6)



(a) EW predominant group (EQ.3b, 5a, 6, 8)

(b) NS predominant group (EQ.1, 2, 8)

Figure 8: Spectral ratios of the surface to bottom at OA downhole site in EW component

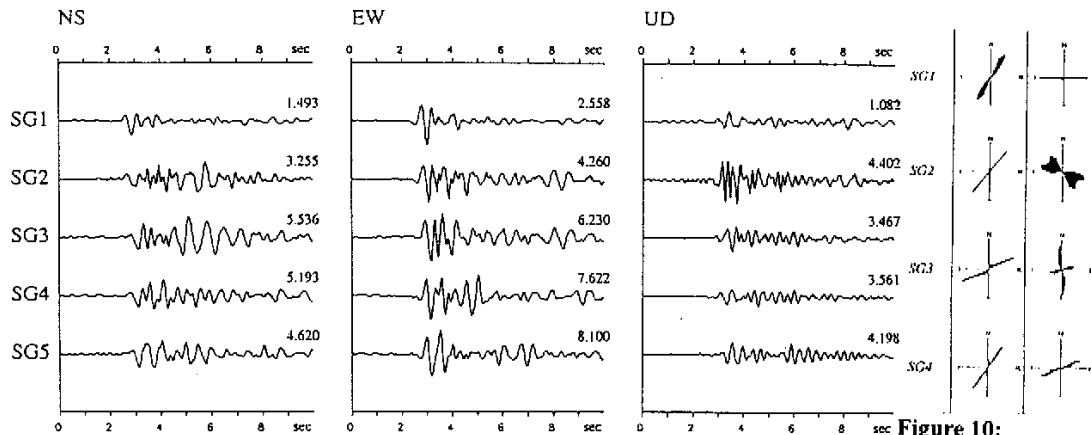


Figure 9: Velocity seismograms on the TKY sediments (EQ.2)

Figure 10:
 principal axis for
 horizontal motion
 $T=2.0-6.0\text{sec}$,
 Left: BPF 0.4-1.0Hz,
 Right: BPF 1.0-2.5Hz

2.2 Typical site effect of buried valley

As seen in Fig.9, the strongest velocity seismograms were recorded during EQ.2. Its S waves were amplified larger at SG3, SG4 and SG5 in a central part of the sedimentary ground. The secondary surface waves are induced by the edge effect. Those waves are traced at a later part of the S wave's principal shock in NS component perpendicular to the sedimentary ground profile.

The principal axis was evaluated by the polarization analysis method [Higashi, S., 1998] for 4 sec duration of the S wave's principal shock at a band pass filter's range from 1.0 to 2.5 Hz. Those were represented in the horizontal plane at each point as seen in Fig.10. The principal axis was almost different at SG2 to SG5 at the sedimentary ground, although most of them were according to the focal radiation pattern in a low frequency region. These results represent that the site effect is mostly affected by a lateral irregularity of the buried valley. Because this site is high contrast ground as indicated impedance ratio factor less than 0.2 between the alluvial clay and the sandstone. Therefore the local site effect is influenced much more remarkably by the underground structure at TKY than by the incident wave field. Furthermore it was recognized that the vertical motion was amplified at SG2 on a steep dipping base layer larger than it on the other gentle dipping.

3. MODELING OF IRREGULARLY LAYERED GROUND

3.1 Horizontal motion spectral amplification at AGK site

As seen in the left hand of Fig.11, the models of deep sediments and basement rock were made by identified geotechnical parameters due to spectral inverse analysis method [Ishida, K., 1984]. Alluvial layer was removed from the model.

Two-dimensional (2D) response analyses due to both antiplane (SH) and inplane (SV) waves incidence by using Aki-Larner (AL) method [Ohori, M., 1990] were conducted in the frequency domain less than 3.5 Hz. One-dimensional (1D) analyses were compared with the two-dimensional (2D) analyses. Incident Ricker wave [Ohori, M., 1990] with the natural frequency of 1.0 Hz was used.

The spectral ratios on OA computed by 2D analysis due to SH were compared with both seismic groups of the NS predominant records (EQ.1, 2 and 8) and the EW predominant records (EQ.3b, 5a, 6 and 8). Fig.12 shows spectral ratios in NS component. The computed spectral ratios almost coincided with the observed ones. But the amplification factor computed by 2D analysis agrees with the observed one around the spectral peak better than those computed by 1D analysis. Thus, 2D analysis due to SH and SV waves incidence are useful to compute irregularly layered ground considering incident wave field.

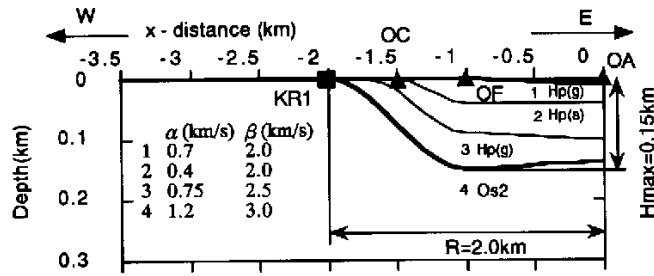


Figure 11: Geotechnical 2D model for AGK

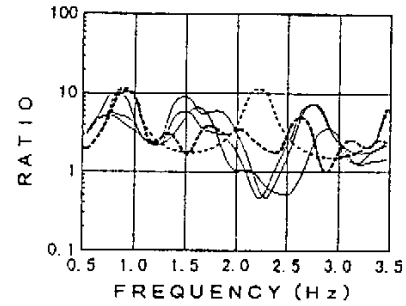


Figure 12:
Comparison of analyzed and observed spectral ratios at OA(-8m/-230m)
Thin line: Observed, Thin broken line: 1D,
Broken line: 2D-SH

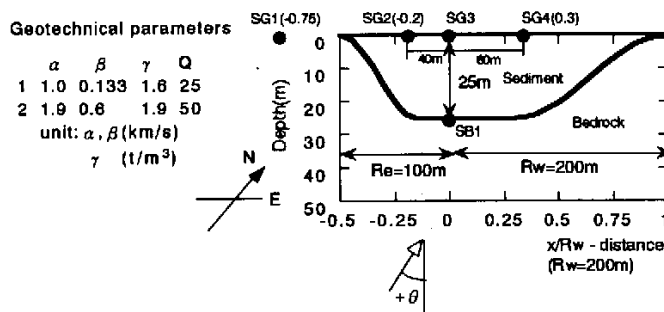


Figure 13: Geotechnical 2D model for TKY

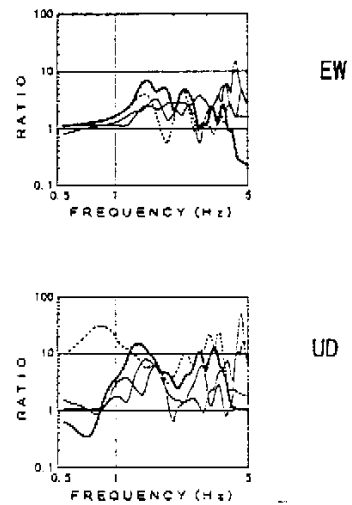


Figure 14: Spectral ratios of SG2/SG1,
Thin line: EQ.2, 6, 5a,
Broken line: vertical incidence 2D,
Bold line: 15 degrees oblique incidence 2D

3.2 Horizontal and vertical motion spectral amplifications at TKY site

2D irregularly layered models were made as for the section of EW direction as seen in Fig.13. The models are shapes of sedimentary basin, which are non-symmetrical 300m long model with 25m deep sediments at both central parts of SG3. 2D analyses were conducted in the frequency domain less than 5.0 Hz.

SG1 is set on the bedrock outcrop at the west edge of the basin. S wave velocity measured by elastic wave's velocity exploration was 900m/s at the surface of the outcrop. This value represents seismic velocity of bedrock at TKY site. Incident Ricker wave's natural frequency was 1.3Hz corresponded to sedimentary layer.

The S wave motion spectral ratios of the surface ground to two reference points of the outcrop SG1 and the downhole SB1 were compared. As a result, it was founded that both amplitudes were almost same. Incident angles for all of recorded earthquakes were estimated by ray theory in the earth's crust structure to consider the phase difference of incident wave field. At this time, the earth's crust structure [Yoshii, T., 1986] estimated by explosive seismic survey in Izu district was used except the S wave velocity of 900m/s in soft bedrock at TKY site.

As seen in Table 4, the seismic incident angles were indicated about 15 degrees from the east and the region less

than 20 degrees from the west. Then 2D analyses due to both of the 15 degree oblique incidence from the east side and the 20 degree oblique incidence from the west side were computed as well as 2D analysis due to the vertical incidence.

Concerning SG2 spectral ratios to a reference point of SG1, the computed ones due to oblique SV wave incidence agree with the observed ones in both components of horizontal EW and vertical UD much better than the computed ones due to vertical SV wave incidence as seen in Fig.14. In the case of 2D analysis due to 20 degrees oblique SV wave incidence from the east, the computed spectral ratios to a reference point of SG1 were different from the computed ones due to the vertical SV wave incidence. Those differences were found apparently in the computed spectral ratios due to 20 degrees oblique SV wave incidence from the west.

Therefore the TKY local site effect is constant and not related to the incident wave field because of the high impedance ratio between the sedimentary and the bedrock layers. But when site effects are evaluated by using spectral ratios to a reference point at the outcrop of bedrock, it is needed to consider the effect of the sedimentary basin on the seismograms at the reference point in accordance with the incident wave's incoming direction and incident angle. Because it is confirmed that the spectral ratios to a reference point at the outcrop of bedrock were different in relation to the source location.

4. CONCLUSIONS

(1) Concerning the spectral ratios between the surface and bottom seismograms of the principal S wave at Kuno, the local site effect was apparently constant in the low frequency region less than 2.5 Hz with respect to the S-wave's predominant component corresponded to the focal radiation pattern and seismic path.

(2) The spectral ratios to a reference point at the bedrock outcrop were different in accordance with the incident wave field even if the spatial separation is less than 100 m in the buried valley at TKY. 2-D response analysis due to oblique S wave incidence agrees to the site amplifications in both horizontal and vertical components. This conclusion leads to the necessity to consider the incident wave field such as the incident angle and the incoming direction in the buried valley.

(3) Local site effects of small and middle sized sedimentary basins, is variable in accordance with the incident wave field. Thus the incident wave field should be considered to evaluate local site effects in its simulation.

5. REFERENCES

- Higashi, S., Sato, K., Yajima, H., Sasaki, S. and Ishikawa, H. (1997), "Underground structure of Kuno-site on the basis of reflection seismic survey", Academic association of earth and planet, p142, B42-P12, (in Japanese).
- Higashi, S., Sato, K., Yajima, H., Sasaki, S. and Ishikawa, H. (1998), "Analysis of incident wave field on Kuno site", The 10th JEES.
- IASPEI/IAEE Joint WG and Japanese National WG (1992), "Proceedings of the International Symposium on the Effect of Surface Geology on Seismic Motion", ESG 1992 Vol II.
- Ishida, K., Sawada, Y., Sato, K. and Yajima, H. (1984), "Concerning a damping of soil - Estimation of Q-value by applying spectral inverse method", The proceeding of the seismological society of Japan, Autumn meeting.
- Kennet, B.L.N. (1988), "Radiation from a Moment-Tensor Source, Seismological Algorithms", pp.427-441.
- Matsuda, T.(1974), "Magnitude and return period of earthquake occurred from active fault", vol. 128, pp.269-283, (in Japanese).
- Ohori, M. (1990), "Seismic response analysis of sedimentary basin by using two-dimensional AL method", Journal of Zisin, vol1165.
- Sato, K., Higashi, S., Shiba, Y., Yajima, H. and Sasaki, S. (1998), "Site amplification and incident wave field at Kuno in Odawara city during 1996 East Yamanashi earthquake", CRIEPI Report U98061, (in Japanese).
- Yoshii, T., Asano, S., Kubota, S., Sasaki, Y., Okada, H., Masuda, T., Murakami, H., Suzuki, S., Moriya, T., Nishide, N. and Inatani, H.(1986), "Detailed Crust Structure in the Izu Peninsula as Revealed by Explosion Seismic Experiments", J. Phys. Earth, 34, Suppl.